Supplementary Material (ESI) for Journal of Materials Chemistry

A Designed Nanoporous Material for Phosphate Removal with High Efficiency

Jie Yang,[a,b] Liang Zhou,[b] Lingzhi Zhao,[b] Hongwei Zhang,[b] Jiani Yin,[c] Guangfeng Wei,[b] Kun Qian,[b] Yunhua Wang,[b] and Chengzhong Yu*[a,b]

[a] ARC Centre of Excellence for Functional Nanomaterials and Australian Institute for Bioengineering and Nanotechnology, The University of Queensland, Brisbane, QLD 4072, Australia.
[b] Department of Chemistry and Shanghai Key Laboratory of Molecular Catalysis and Innovative Materials Fudan University, Shanghai, 200433 (P. R. China)
[c] Department of Biology
Fudan University, Shanghai, 200433 (P. R. China)

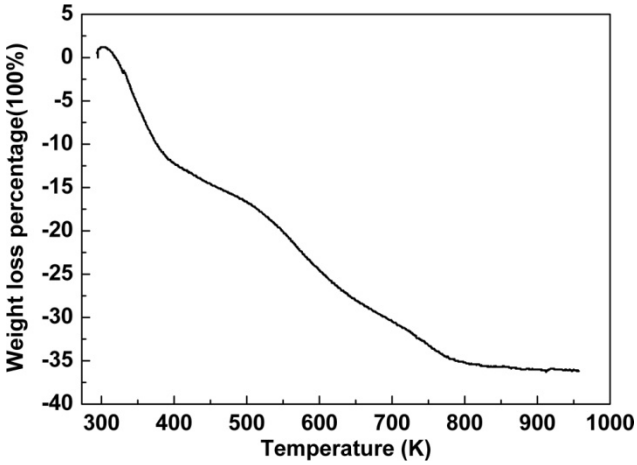

Fig. S1. Thermogravimetric Analysis (TGA) profile of La_{100}SBA-15.

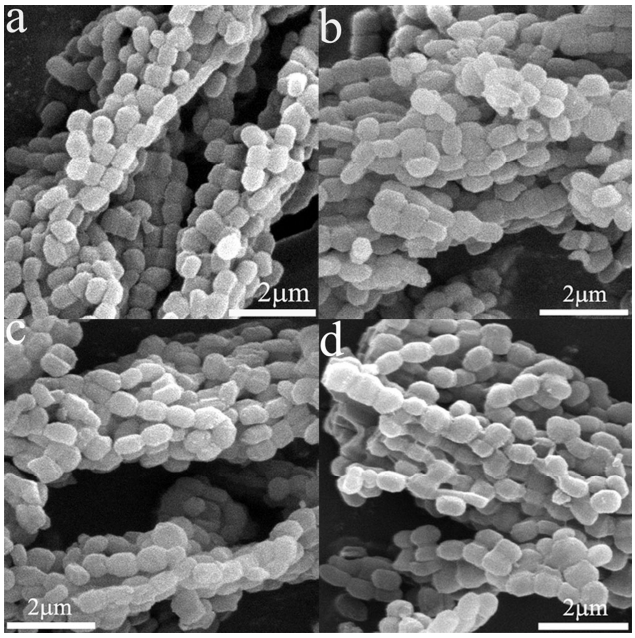

Fig. S2. SEM images of (a) SBA-15, (b) La_{40}SBA-15, (c) La_{80}SBA-15 and (d) La_{100}SBA-15.

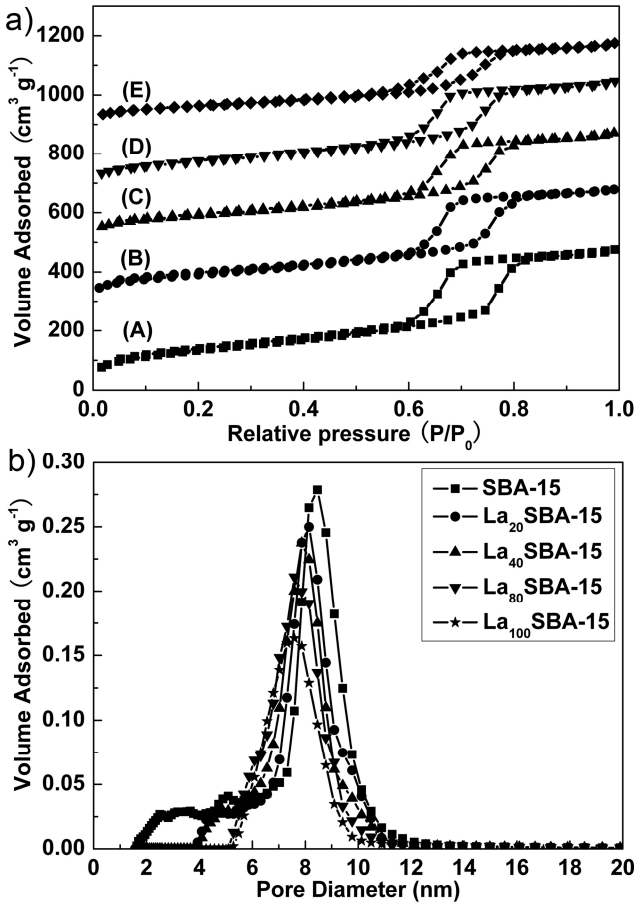

Fig. S3. (a) Nitrogen adsorption-desorption isotherms for La_XSBA-15 materials: (A) SBA-15, (B) $La_{20}SBA$-15, (C) $La_{40}SBA$-15, (D) $La_{80}SBA$-15, and (E) $La_{100}SBA$-15; (b) The pore size distribution curves of samples calculated from the adsorption branches using the Density Functional Theory (DFT) method.

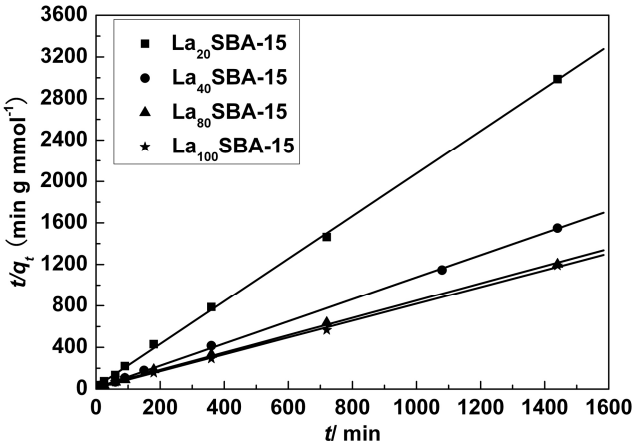

Fig. S4. The plot of t/q_t versus t using linear regression.

Note:

Take into account the initial adsorption rate ν_0 (mmolg^{-1}min^{-1})

$$\nu_0 = k \cdot q_{eq}^2 \quad (1)$$

Equation 1 can be rearranged to obtain

$$\frac{t}{q_t} = \frac{1}{\nu_0} + \frac{1}{q_{eq}} t \quad (2)$$

The values of q_{eq}, ν_0 and rate constant k can be determined experimentally by plotting t/q_t versus t.

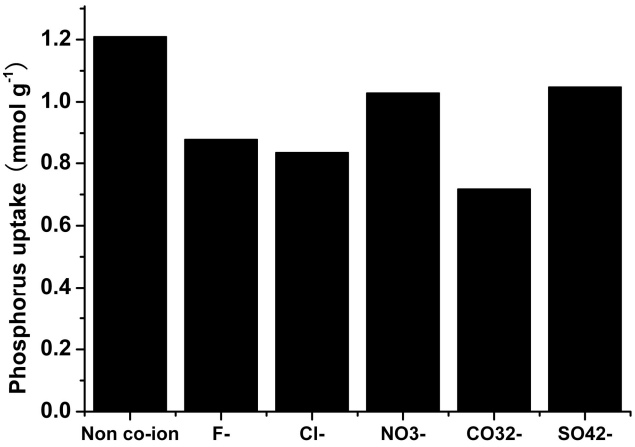

Fig. S5. Effect of foreign anions on adsorption capacity. Sorbent dosage: 0.050 g/50 mL; phosphate concentration: 50 mg/L; foreign anions concentrations: 400 mg/L; temperature: 25°C; stirring speed 120 r/min.

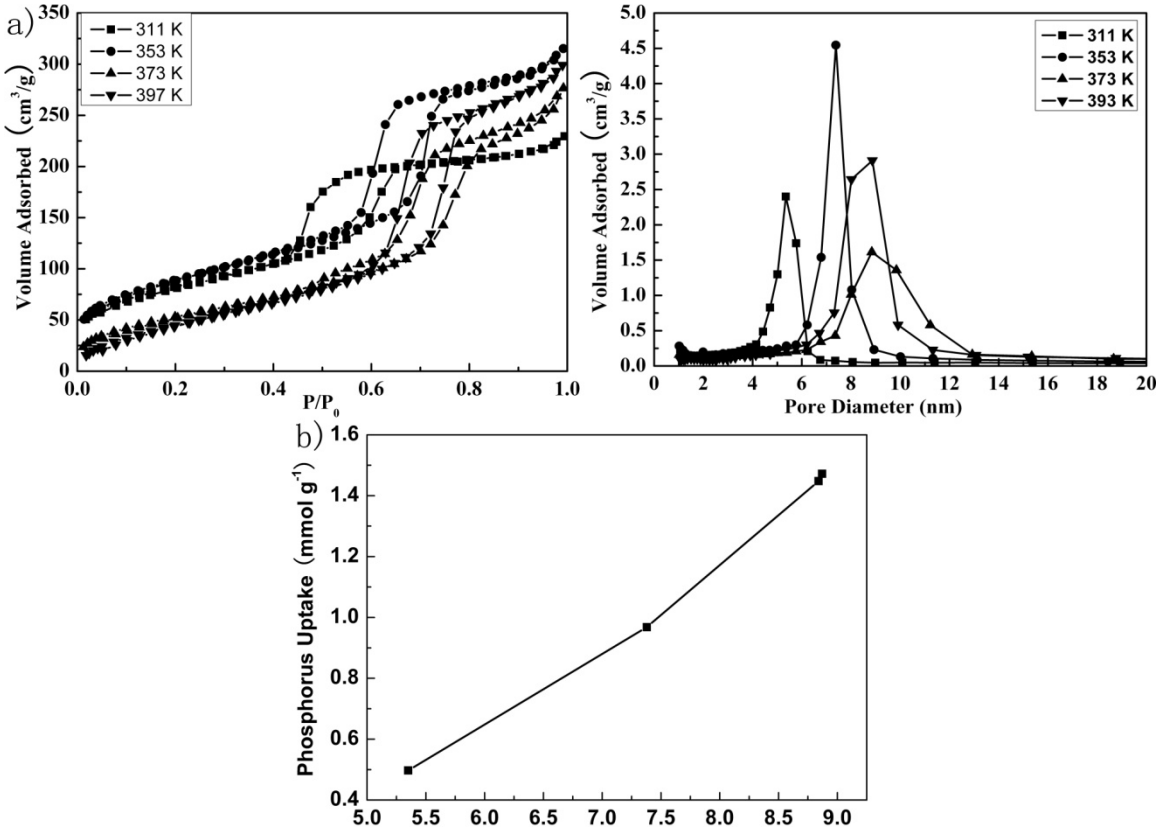

Fig. S6. (a) Nitrogen adsorption-desorption isotherms (left) and the pore size distribution curves (right) of La_{100}SBA-15 materials with different pore size; (b) phosphate adsorption test.Phosphorus adsorption capacities of La_{100}SBA-15 materials with different pore size.

Note: the preparation method of La_{100}SBA-15 materials with different pore size: SBA-15 materials with different pore sizes (5.35, 7.38, 8.84, and 8.87 nm) were synthesized by changing the hydrothermal treatment temperatures (311, 353, 373 and 393 K, respectively). The other synthesis procedures and the following steps of La impregnation are the same as described in producing normal La_{100}SBA-15 materials.

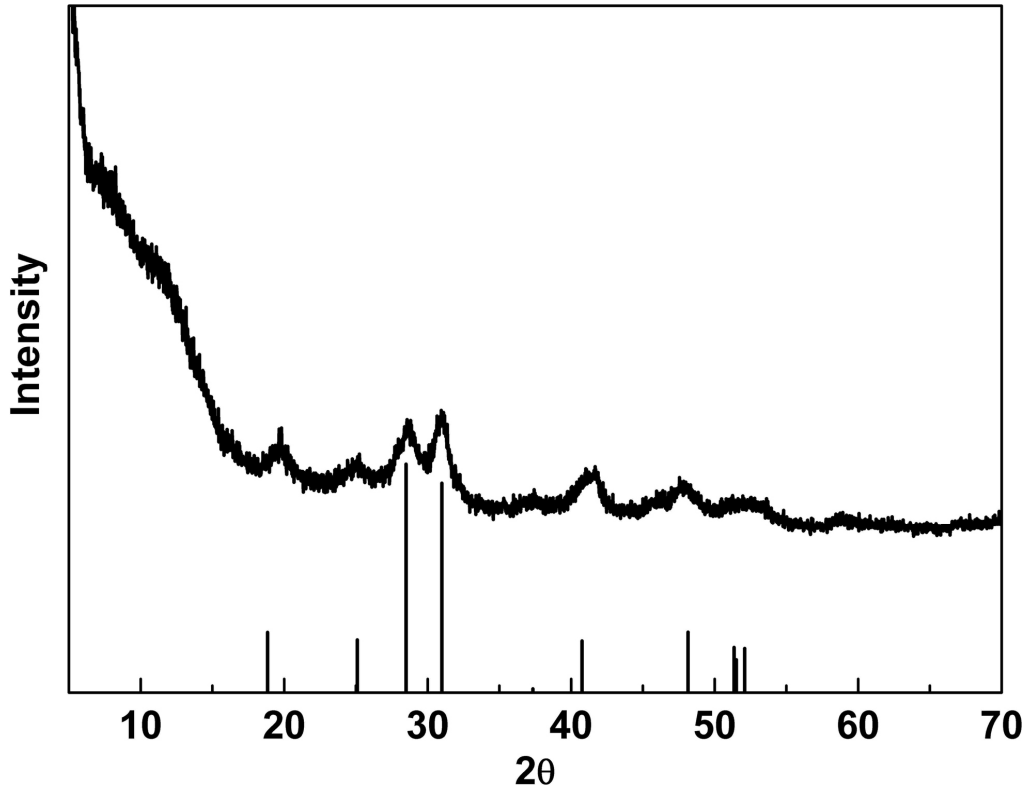

Fig. S7. The wide-angle XRD pattern of La_{100}SBA-15 material after adsorption.

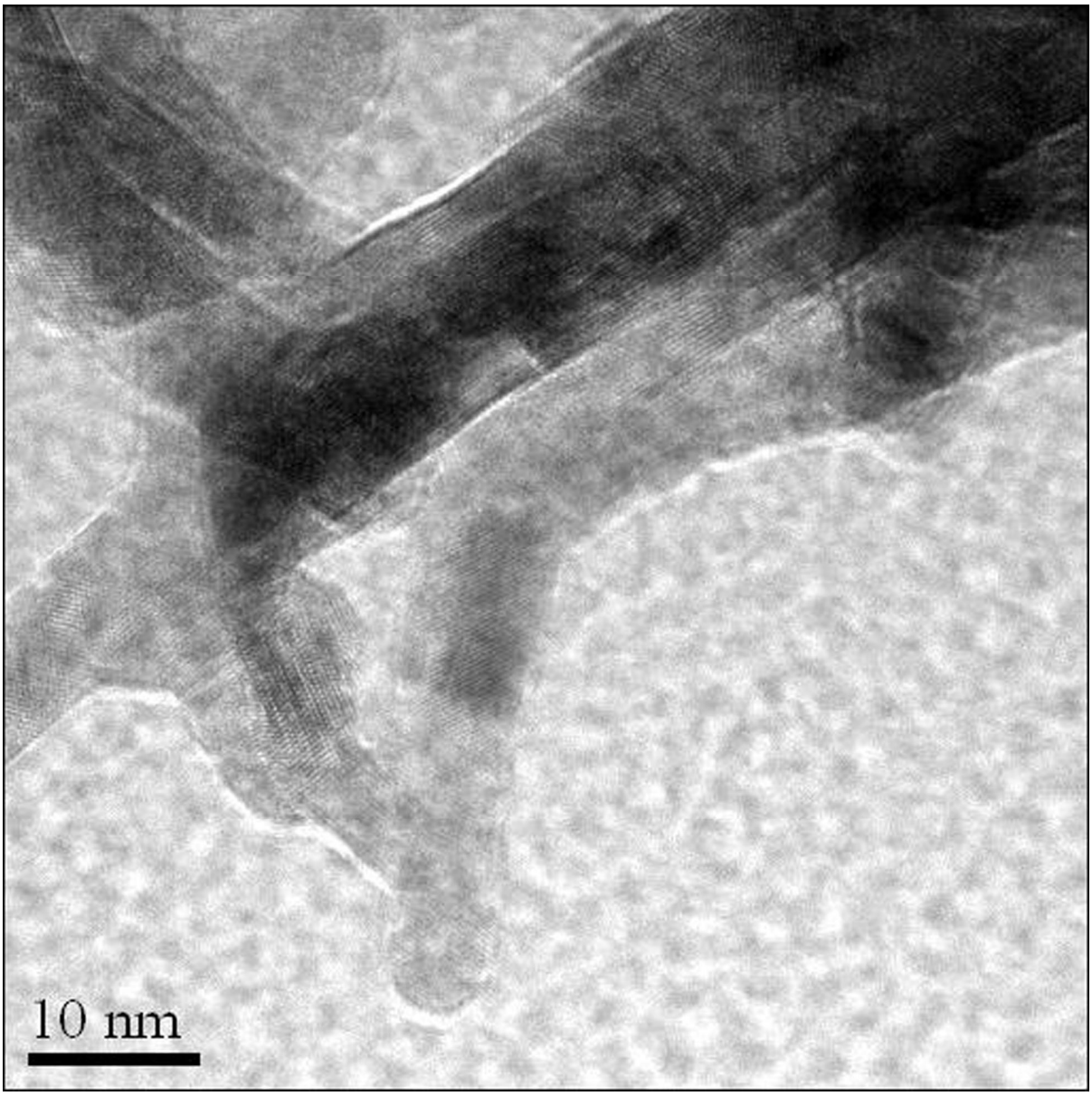

Fig. S8. The HRTEM image of needle-like crystals of La_{100}SBA-15 material.

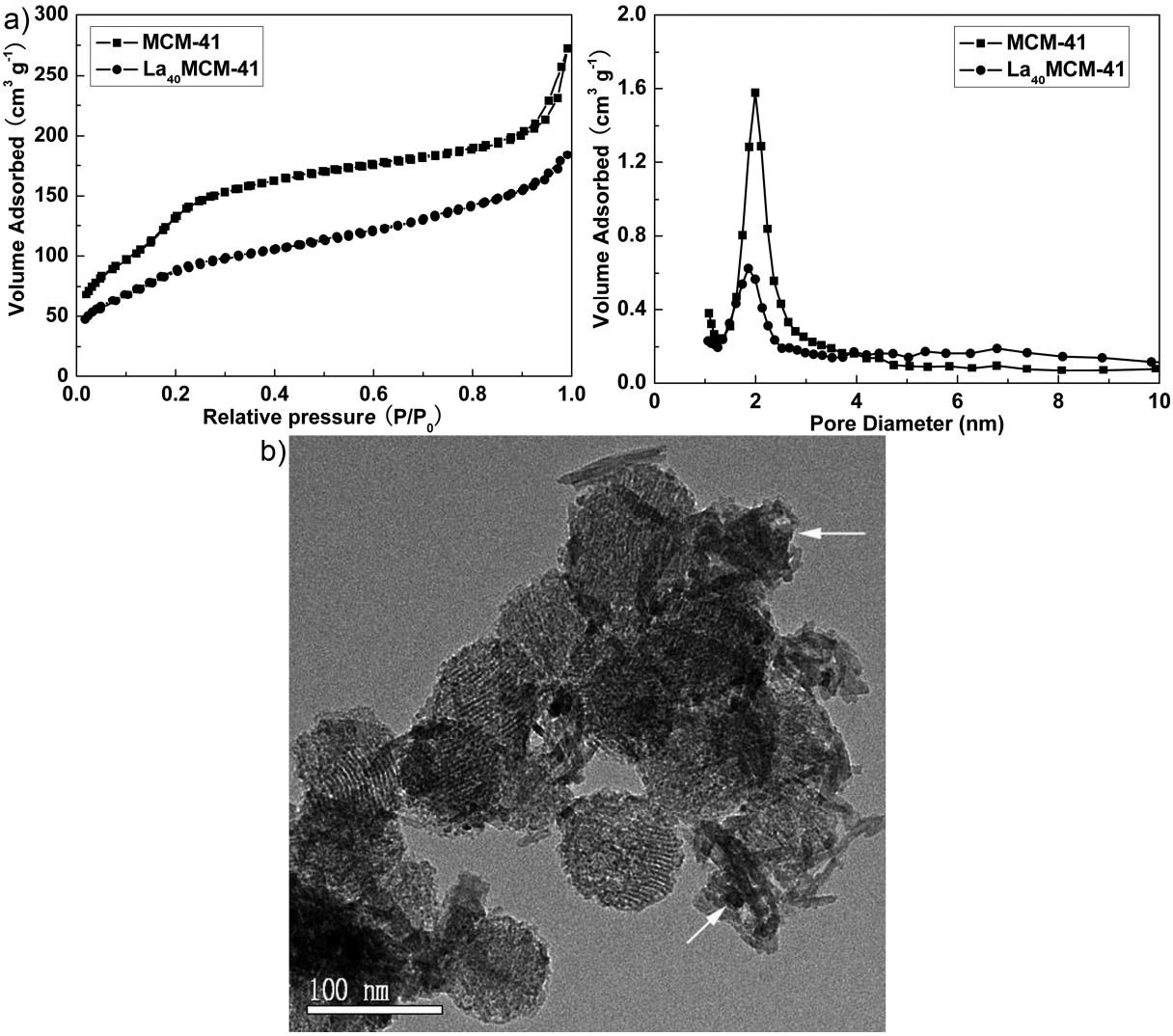

Fig. S9. (a) Nitrogen adsorption-desorption isotherms and the pore size distribution curves of MCM-41 and La_{40}MCM-41; (b) TEM image of La_{40}MCM-41 after 24 h phosphate adsorption test.

Note: The surface area, pore volume and pore size of La_{40}MCM-41 (321 m^2/g, 0.28 cm^3/g and 1.86 nm, respectively) are smaller than that of MCM-41 (556 m^2/g, 0.42 cm^3/g and 1.99 nm, respectively), which can be attributed to the impregnation of La components into the mesopores. The TEM image (Figure S3b) of La_{40}MCM-41 after 24 h phosphate adsorption shows that some of the LaP species form in the outer part of La_{40}MCM-41 particles with a rod-like morphology (as indicated by white arrows), however the diameters of the rods are much larger compared to the pore size of La_{40}MCM-41. The kinetic parameter *k* of La-MCM-41 is smaller than that of La-SBA-15, indicating that the adsorption of phosphates in La-SBA-15 is faster than in La-MCM-41 with a relatively smaller pore channel size. The high value of empirical constant *b* suggests that La-MCM-41 is more suitable for the adsorption of phosphates with a low concentration.

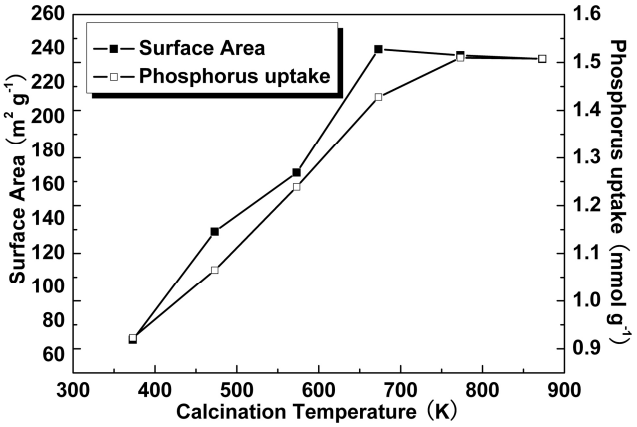

Fig. S10. Surface area and phosphorus adsorption capacities with different calcinations temperature.

Table S1. Summary of properties of La_XSBA-15 materials.

samples	x	d spacing (nm)	S_{BET} (m^2/g)	D_{DFT} (nm)	V (cm^3/g)
SBA-15	0	9.72	476	8.46	0.74
La_{20}SBA-15	20	9.39	333	8.15	0.59
La_{40}SBA-15	40	9.50	326	7.87	0.57
La_{80}SBA-15	80	9.61	285	7.59	0.54
La_{100}SBA-15	100	9.72	227	7.58	0.43

Note: d spacing is calculated from its first (100) diffraction peak; S_{BET} is the surface area calculated using Brumauer-Emmett-Teller (BET) method; D_{DFT} is the pore diameter calculated using Density Functional Theory (DFT) method; and V is the total pore volume.

Table S2. Langmuir, Freundlich parameters and kinetic paremeters for phosphate adsorption on each sample.

samples	Pesudo-second-order kinetic modal		Langmuir modal				Freundlich modal		
	[§]R	[§]k (g/mmol·min)	[†]R^2	[†]b (L/mmol)	[†]Q_{max} (mmol/g)	P/La	[¶]R^2	[¶]K (mmol$^{(1-n)}$L^{n}g^{-1})	[¶]n
La_{20}SBA-15	0.999	0.190	0.991	22.66	0.529	1.231	0.967	0.523	5.877
La_{40}SBA-15	0.999	0.099	0.989	20.81	0.938	1.168	0.945	0.952	4.538
La_{80}SBA-15	0.999	0.039	0.981	23.26	1.307	0.920	0.947	1.232	6.100
La_{100}SBA-15	0.999	0.066	0.975	17.14	1.362	0.812	0.883	1.360	3.971
La_{40}MCM-41	0.998	0.027	0.994	110.56	0.767	0.955	0.958	0.821	7.307

[§] kinetic parameters: R is the correlation coefficients, k is the rate constant of the pseudo second-order kinetic model (g/mmol·min).

[†] Langmuir parameters: R^2 is the correlation coefficients, Q^{max} is the maximum adsorption amount (mmol/g), and b is Langmuir constant (L/mmol).

[¶] Freundlich paremeters: R^2 is the correlation coefficients, K (mmol(1-n)Lng-1) and n are empirical constants.

The $LaPO_4$ species crystallization analysis for mesoporous structure using classic crystallization theory

1. Homogeneous Nucleation.

In a homogeneous solution without any foreign substrates, a nucleus can form spontaneously in a bulk of supersaturated system due to the fluctuation of energy. Two energy terms are involved in the growth of the nucleus: one is the volume excess free energy, ΔG_V; the other is the interfacial surface excess free energy, ΔG_S. The total excess free energy of the system, ΔG_{HOMO} is the sum of these two energy terms:

$$\Delta G_{HOMO} = \Delta G_V + \Delta G_S \tag{1}$$

Suppose a spherical shape of the nuclei, with radius r, for a given volume free energy change per unit volume, ΔG_V, and the interfacial tension, $\sigma_{n\text{-}l}$, eq 1 can be expressed as follows:

$$\Delta G = \frac{4\pi r^3}{3}\Delta G_V + 4\pi r^2 \sigma_{n-l} \tag{2}$$

Note that ΔG_V is a negative quantity. The, r, radius of the nuclei is a key parameter responsible for the system free energy change. By differentiating eq 2 with r, and then set it as zero, a critical nuclei size r^* is obtained,

$$r^* = -\frac{2\sigma_{n-l}}{\Delta G_V} \tag{3}$$

The critical nuclei size, r^*, is responsible for the turning point of the system free energy change, ΔG. If a nuclei size, r, is less than r^*, then ΔG will increase with the growth of the nuclei, hence the growing is thermodynamically unfavorable. If r is larger than r^*, ΔG would decrease with the growth of the nuclei, then the growing is thermodynamically favorable. Such nucleus ($r \geq r^*$) becomes a crystallization center.

2. Heterogeneous Nucleation.

When a foreign substrate is presented in the supersaturated solution and a nucleation occurs on this foreign substrate, this process is called "heterogeneous nucleation". Assume that the nucleus is in the form of a spherical cap on the substrate, the volume excess free energy, ΔG_V is the multiple of the actual cap volume, V_{cap}, and the free energy change per volume, ΔG_v,

$$\Delta G_V = \Delta G_v \cdot V_{cap} \tag{4}$$

V_{cap} can be calculated as follows:

$$V_{cap} = \frac{\pi r^3}{3}\left(2 - 3\cos\theta + \cos^3\theta\right) \tag{5}$$

θ is the contact angle that the nucleus spreads on the substrate. And then interfacial surface excess energy, ΔG_S is given by

$$\Delta G_S = 4\pi r^2 S_{cap}\sigma_{n-l} + \pi r^2 \sin^2\theta\left(\sigma_{n-s} - \sigma_{s-l}\right) \tag{6}$$

The surface area of the cap is denoted by S_{cap}. And $\sigma_{n\text{-}l}$ is the nuclei-liquid interfacial energy per unit area of the new $LaPO_4$ surface created. $\sigma_{n\text{-}s}$ and $\sigma_{s\text{-}l}$ are the nuclei-substrate and substrate-liquid interfacial energy per unit area. The relation among the three interfacial energy terms is given by the following:

$$\sigma_{s-l} = \sigma_{n-s} + \sigma_{n-l}\cos\theta \tag{7}$$

Thus, the total free energy changed in the heterogeneous nucleation, ΔG_{HETERO} can be obtained by combining eqs 4-7 as

$$\Delta G_{HETERO} = \left(\frac{4\pi r^3}{3}\Delta G_V + 4\pi r^2 \sigma_{n-l}\right)\cdot f(\theta) \tag{8a}$$

$$f(\theta) = \frac{1}{4}(2 - 3\cos\theta + \cos^3\theta) \tag{8b}$$

The total free energy excess in heterogeneous nucleation eq 8a is very much similar to that in the homogeneous nucleation, eq 2. The only extra term in heterogeneous nucleation is the $f(\theta)$ function, accountable for the effect of the contact angle of the $LaPO_4$ nuclei on its substrate. So, the relation between the homogeneous and heterogeneous nucleation can be simplified as follows:

$$\Delta G_{HETERO} = \Delta G_{HOMO} \cdot f(\theta) \tag{9}$$

Since $f(\theta)$ is a factor less than 1, $\Delta G_{\mathrm{HETERO}}$ is always less than ΔG_{HOMO}. So heterogeneous nucleation is much easier to form comparing homogeneous nucleation, given the lower activation energy for the change. For a given system of a substrate, the contact angle θ is a constant, and so is the function $f(\theta)$. Then an important conclusion can be made that the critical nuclei size, r^*, of heterogeneous nucleation is the same as that of the homogeneous process. So we can simply use eq 3 derived from homogeneous situation to get r^* of the real system of $LaPO_4$ heterogeneously nucleated from SBA-15 substrates. The free energy per one cell volume is as follows:

$$\Delta G_v = \frac{\Delta G_V}{N_A \cdot V_m} \tag{10}$$

N_{A} is Avogadro's number and V_{m} is the molecular volume of lanthanum phosphate ($LaPO_4$) lattice cell, 425.26Å^3, obtained from its crystal structure. From eqs 3 and 10, we get

$$r^* = 0.046\sigma_{n-l}(nm) \tag{11}$$

In this study, we estimated that

$$0.93nm < r^* < 4.44nm \tag{12}$$

Thus the value of $\sigma_{\mathrm{n\text{-}l}}$ can be calculated in the range

$$20.21mJ/m^2 < \sigma_{n-l} < 96.52mJ/m^2 \tag{13}$$